

Multi-wavelength coherent transmission using an optical frequency comb as a local oscillator

JUNED N. KEMAL,¹ JOERG PFEIFLE,¹ PABLO MARIN-PALOMO,¹ M. DESEADA GUTIERREZ PASCUAL,³ STEFAN WOLF,¹ FRANK SMYTH,³ WOLFGANG FREUDE,^{1,2} AND CHRISTIAN KOOS^{1,2,*}

¹*Institute of Photonics and Quantum Electronics (IPQ), Karlsruhe Institute of Technology (KIT), Germany*

²*Institute of Microstructure Technology (IMT), Karlsruhe Institute of Technology (KIT), Germany*

³*Pilot Photonics Ltd., Ireland*

*christian.koos@kit.edu

Abstract: Steadily increasing data rates of optical interfaces require spectrally efficient coherent transmission using higher-order modulation formats in combination with scalable wavelength-division multiplexing (WDM) schemes. At the transmitter, optical frequency combs (OFC) lend themselves to particularly precise multi-wavelength sources for WDM transmission. In this work we demonstrate that these advantages can also be leveraged at the receiver by using an OFC as a highly scalable multi-wavelength local oscillator (LO) for coherent detection. In our experiments, we use a pair of OFC that rely on gain switching of injection-locked semiconductor lasers both for WDM transmission and intradyne reception. We synchronize the center frequency and the free spectral range of the receiver comb to the transmitter, keeping the intradyne frequencies for all data channels below 15 MHz. Using 13 WDM channels, we transmit an aggregate line rate (net data rate) of 1.104 Tbit/s (1.032 Tbit/s) over a 10 km long standard single mode fiber at a spectral efficiency of 5.16 bit/s/Hz. To the best of our knowledge, this is the first demonstration of coherent WDM transmission using synchronized frequency combs as light source at the transmitter and as multi-wavelength LO at the receiver.

© 2016 Optical Society of America

OCIS codes: (060.0060) Fiber optics and optical communications; (060.1660) Coherent communications; (140.3520) Lasers, injection-locked; (060.4510) Optical communications; (200.4650) Optical interconnects

References and links

1. P. Winzer, "Beyond 100G Ethernet," *IEEE Commun. Mag.* **48**(7), 26–30 (2010).
2. C. R. Cole, "100-Gb/s and beyond transceiver technologies," *Opt. Fiber Technol.* **17**(5), 472–479 (2011).
3. S. Gringeri, E. B. Basch, and T. J. Xia, "Technical considerations for supporting data rates beyond 100 Gb/s," *IEEE Commun. Mag.* **50**(2), S21–S30 (2012).
4. D. A. B. Miller, "Device requirements for optical interconnects to silicon chips," *Proc. IEEE* **97**(7), 1166–1185 (2009).
5. J. Geyer, C. R. Doerr, M. Aydinlik, N. Nadarajah, A. Caballero, C. Rasmussen, and B. Mikkelsen, "Practical implementation of higher order modulation beyond 16-QAM," in *Optical Fiber Communication Conference*, OSA Technical Digest (online) (OSA, 2015), paper Th1B.1.
6. D. Hillerkuss, R. Schmogrow, T. Schellinger, M. Jordan, M. Winter, G. Huber, T. Vallaitis, R. Bonk, P. Kleinow, F. Frey, M. Roeger, S. Koenig, A. Ludwig, A. Marculescu, J. Li, M. Hoh, M. Dreschmann, J. Meyer, S. Ezra, N. Ben, N. Narkiss, B. Nebendahl, F. Parmigiani, P. Petropoulos, B. Resan, A. Oehler, K. Weingarten, T. Ellermeyer, J. Lutz, M. Moeller, M. Huebner, J. Becker, C. Koos, W. Freude, and J. Leuthold, "26 Tbit s-1 line-rate super-channel transmission utilizing all-optical fast Fourier transform processing," *Nat. Photonics* **5**(6), 364–371 (2011).
7. D. Hillerkuss, R. Schmogrow, M. Meyer, S. Wolf, M. Jordan, P. Kleinow, N. Lindenmann, P. C. Schindler, A. Melikyan, X. Yang, S. Ben-Ezra, B. Nebendahl, M. Dreschmann, J. Meyer, F. Parmigiani, P. Petropoulos, B. Resan, A. Oehler, K. Weingarten, L. Altenhain, T. Ellermeyer, M. Moeller, M. Huebner, J. Becker, C. Koos, W. Freude, and J. Leuthold, "Single-laser 32.5 Tbit/s Nyquist WDM transmission," *J. Opt. Commun. Netw.* **4**(10), 715–723 (2012).

8. E. Temprana, E. Myslivets, B. P. P. Kuo, L. Liu, V. Ataie, N. Alic, and S. Radic, "Overcoming Kerr-induced capacity limit in optical fiber transmission," *Science* **348**(6242), 1445–1448 (2015).
9. E. Temprana, V. Ataie, B. P. P. Kuo, E. Myslivets, N. Alic, and S. Radic, "Dynamic reconfiguration of parametric frequency comb for superchannel and flex-grid transmitters," in *European Conference on Optical Communication (ECOC, 2014)*, paper P.3.14.
10. C. Zhangyuan, Z. Paikun, L. Juhao, X. Yingying, W. Zhongying, C. Xin, C. Yuanxiang, and H. Yongqi, "Key technologies for elastic optical networks," in *13th International Conference on Optical Communications and Networks (ICOON, 2014)*, paper S32.3.
11. J. Pfeifle, V. Brasch, M. Laueremann, Y. Yu, D. Wegner, T. Herr, K. Hartinger, P. Schindler, J. Li, D. Hillerkuss, R. Schmogrow, C. Weimann, R. Holzwarth, W. Freude, J. Leuthold, T. J. Kippenberg, and C. Koos, "Coherent terabit communications with microresonator Kerr frequency combs," *Nat. Photonics* **8**(5), 375–380 (2014).
12. C. Weimann, P. C. Schindler, R. Palmer, S. Wolf, D. Bekele, D. Korn, J. Pfeifle, S. Koeber, R. Schmogrow, L. Alloati, D. Elder, H. Yu, W. Bogaerts, L. R. Dalton, W. Freude, J. Leuthold, and C. Koos, "Silicon-organic hybrid (SOH) frequency comb sources for terabit/s data transmission," *Opt. Express* **22**(3), 3629–3637 (2014).
13. J. Pfeifle, V. Vujicic, R. T. Watts, P. C. Schindler, C. Weimann, R. Zhou, W. Freude, L. P. Barry, and C. Koos, "Flexible Terabit/s Nyquist-WDM super-channels using a gain-switched comb source," *Opt. Express* **23**(2), 724–738 (2015).
14. P. Marin, J. Pfeifle, M. Karpov, P. Trocha, R. Rosenberger, K. Vijayan, S. Wolf, J. N. Kemal, A. Kordts, M. Pfeiffer, V. Brasch, W. Freude, T. Kippenberg, and C. Koos, "50 Tbit/s massively parallel WDM transmission in C and L band using interleaved cavity-soliton Kerr combs," in *Conference on Lasers and Electro-Optics (OSA, 2016)*, paper STu1G.1.
15. V. Ataie, E. Temprana, L. Liu, E. Myslivets, B. P.-P. Kuo, N. Alic, and S. Radic, "Ultrahigh count coherent WDM channels transmission using optical parametric comb-based frequency synthesizer," *J. Lightwave Technol.* **33**(3), 694–699 (2015).
16. P. J. Delfyett, S. Gee, M.-T. Choi, H. Izadpanah, W. Lee, S. Ozharar, F. Quinlan, and T. Yilmaz, "Optical frequency combs from semiconductor lasers and applications in ultrawideband signal processing and communications," *J. Lightwave Technol.* **24**(7), 2701–2719 (2006).
17. X. Yi, N. K. Fontaine, R. P. Scott, and S. J. B. Yoo, "Tb/s Coherent optical OFDM systems enabled by optical frequency Combs," *J. Lightwave Technol.* **28**(14), 2054–2061 (2010).
18. N. K. Fontaine, G. Raybon, B. Guan, A. L. Adamiecki, P. Winzer, R. Ryf, A. Konczykowska, F. Jorge, J.-Y. Dupuy, L. L. Buhl, S. Chandrasekhar, R. Delbue, P. Pupaiaikis, and A. Sureka, "228-GHz coherent receiver using digital optical bandwidth interleaving and reception of 214-GBd (856-Gb/s) PDM-QPSK," in *European Conference and Exhibition on Optical Communication, OSA Technical Digest (online) (OSA, 2012)*, paper Th.3.A.1.
19. N. K. Fontaine, R. P. Scott, L. Zhou, F. M. Soares, J. P. Heritage, and S. J. B. Yoo, "Real-time full-field arbitrary optical waveform measurement," *Nat. Photonics* **4**(4), 248–254 (2010).
20. J. N. Kemal, J. Pfeifle, P. Marin, M. D. Gutierrez Pascual, F. Smyth, W. Freude, and C. Koos, "Parallel multi-wavelength intradyne reception using an optical frequency comb as a local oscillator," in *European Conference and Exhibition of Optical Communication (ECOC, 2015)*, paper P.4.18.
21. P. M. Anandarajah, R. Maher, Y. Xu, S. Latkowski, J. O'Carroll, S. G. Murdoch, R. Phelan, J. O'Gorman, and L. Barry, "Generation of coherent multicarrier signals by gain switching of discrete mode lasers," *IEEE Photonics J.* **3**(1), 112–122 (2011).
22. R. Zhou, S. Latkowski, J. O'Carroll, R. Phelan, L. P. Barry, and P. Anandarajah, "40 nm wavelength tunable gain-switched optical comb source," *Opt. Express* **19**(26), B415–B420 (2011).
23. G. Yabre, H. de Waardt, H. P. A. Van den Boom, and G.-D. Khoe, "Noise characteristics of single-mode semiconductor lasers under external light injection," *IEEE J. Quantum Electron.* **36**(3), 385–393 (2000).
24. M. D. G. Pascual, R. Zhou, F. Smyth, P. M. Anandarajah, and L. P. Barry, "Software reconfigurable highly flexible gain switched optical frequency comb source," *Opt. Express* **23**(18), 23225–23235 (2015).
25. R. Zhou, P. M. Anandarajah, D. Gutierrez Pascual, J. O'Carroll, R. Phelan, B. Kelly, and L. P. Barry, "Monolithically integrated 2-section lasers for injection locked gain switched comb generation," in *Optical Fiber Communication Conference, OSA Technical Digest (online) (OSA, 2014)*, paper Th3A.3.
26. R. Zhou, T. N. Huynh, V. Vujicic, P. M. Anandarajah, and L. P. Barry, "Phase noise analysis of injected gain switched comb source for coherent communications," *Opt. Express* **22**(7), 8120–8125 (2014).
27. R. Noé, W. B. Sessa, R. Welter, and L. G. Kazovsky, "New FSK phase-diversity receiver in a 150 Mbit/s coherent optical transmission system," *Electron. Lett.* **24**(9), 567–568 (1988).
28. F. Chang, K. Onohara, and T. Mizuochi, "Forward error correction for 100 G transport networks," *IEEE Commun. Mag.* **48**(3), S48–S55 (2010).
29. OptSim, (Synopsys, Inc., 2016), <https://optics.synopsys.com/rsoft/rsoft-system-network-optim.html>.
30. K. Kikuchi, "Characterization of semiconductor-laser phase noise and estimation of bit-error rate performance with low-speed offline digital coherent receivers," *Opt. Express* **20**(5), 5291–5302 (2012).
31. TL5000DCJ, (OCLARO, 2016), <http://www.oclaro.com/product/tl5000dcj>
32. MAFA 1023, (emcore, 2016), <http://emcore.com/wp-content/uploads/2016/02/MAFA-1000-Series.pdf>
33. J. Pfeifle, A. Kordts, P. Marin, M. Karpov, M. Pfeiffer, V. Brasch, R. Rosenberger, J. Kemal, and S. Wolf, "Full C and L-Band Transmission at 20 Tbit / s Using Cavity-Soliton Kerr Frequency Combs," in *CLEO: 2015 Postdeadline Paper Digest (OSA, 2015)*, paper JTH5C.8.

1. Introduction

Driven by increasing pressure on data-center and telecom operators to handle escalating traffic, optical interfaces with data rates of 400 Gbit/s are currently being standardized, and Tbit/s interfaces are already under discussion [1–3]. To keep symbol rates compliant with the electrical bandwidth of energy-efficient CMOS driver circuitry, a technical implementation of such interfaces requires higher-order modulation formats along with parallel transmission on a multitude of wavelength channels [4,5]. In this context, optical frequency combs (OFC) lend themselves to particularly attractive sources to generate a number of well-defined wavelength-division multiplexing (WDM) carriers in a single chip-scale device. Unlike the carriers derived from a bank of individual lasers, the tones of a comb are intrinsically equidistant in frequency and can be controlled by just two parameters – by the center frequency and by the free spectral range (FSR). This enables transmission of orthogonal frequency division multiplexing (OFDM) [6] or of Nyquist-WDM [7] signals at highest spectral efficiency. In addition, stochastic frequency variations of the various comb lines are strongly correlated, which considerably facilitates compensation of impairments caused by nonlinearities of the transmission fiber in WDM links [8]. OFC with tunable center frequency and tunable FSR are of particular interest, enabling dynamic adaption of the symbol rate and the carrier spacing to the bandwidth demand and the required reach [9,10]. Such devices might be key to next-generation flex-grid networks as recommended by the International Telecommunication Union (ITU), ITU-T G.694.1.

OFC have previously been used as optical sources for WDM transmission, and a variety of experiments demonstrate Tbit/s line rates, both with integrated chip-scale devices [11–14] and with systems that rely on conventional setups of discrete components [6,7,15]. However, most of these experiments still employ a high-quality single-wavelength external-cavity laser (ECL) as a local oscillator (LO) for channel-by-channel demodulation of the coherent signals. Simultaneous reception of all data channels in a practical transmission system would require an array of stabilized LO lasers corresponding to the number of transmitted carriers. The associated technical effort is considerable, in particular when it comes to large channel numbers. For massively parallel WDM systems, it might hence be highly attractive to leverage the scalability advantages of optical frequency combs also at the receiver side. In this context, different schemes have been discussed, using either phase-locked [16] or free-running [17,18] LO combs. To achieve phase locking, dual-mode injection locking of a semiconductor laser was used [16]. However, this scheme does not allow for significant tuning of the FSR and is only applicable to comb sources which can be injection locked. Moreover, the associated experimental demonstrations were so far limited to data transmission over a single WDM channel at a comparatively low data rate of 316.5 Mbit/s using simple on-off-keying (OOK) as a modulation format. Regarding free-running LO combs, spectrally sliced signal processing was demonstrated to be a viable scheme for wideband coherent detection [19]. This scheme was used for reception of orthogonal frequency division multiplexing (OFDM) signals. In a first experiment [17], the OFDM signal was generated by modulating identical data on 32 comb lines spaced by approximately 10 GHz. A subset of spectral slices carrying approximately 100 Gbit/s of data was then successfully detected using an LO that consists of only two lines, spaced by approximately 40 GHz. In another work [18], spectrally sliced detection was used to receive a high-speed 214 GBd single-carrier dual-polarization quadrature phase shift keying (QPSK) signal within a bandwidth of 228 GHz, leading to a data rate of 856 Gbit/s and a spectral efficiency of 3.51 bit/s/Hz. In this scheme, the data signal was generated by advanced temporal interleaving using high-speed LiNbO₃ modulators, hence exploiting the scalability advantages of OFC only at the receiver side. In general, OFC-supported spectrally sliced detection represents a very powerful approach that allows a full reconstruction of arbitrary optical waveforms at

bandwidths beyond those accessible by electronic signal processing. However, the scheme requires arrays of parallelized high-speed digitizers that are precisely synchronized, thereby limiting scalability with respect to larger channel counts. Moreover, the digital signal processing (DSP) required for waveform reconstruction goes significantly beyond that of conventional coherent receivers. This leads to considerable technical complexity that still appears prohibitive for implementation in current receiver systems.

In this work we demonstrate that OFC can be used as multi-tone LO for simultaneous coherent reception of WDM signals using arrays of independent digitizers and conventional DSP. In our experiment, we use a pair of OFC that rely on switching the gain of injection-locked semiconductor lasers for both WDM transmission and intradyne reception. We synchronize the center frequency and the free spectral range of the receiver comb to the transmitter, keeping the intradyne frequencies for all data channels below 15 MHz. In extension of our previous results [20], we use 13 WDM carriers to transmit an aggregate line rate (net data rate) of 1.104 Tbit/s (1.032 Tbit/s) over a 10 km long standard single mode fiber. Using two polarizations and a combination of QPSK and 16-state quadrature amplitude modulation (16QAM) to encode the data, we achieve a net spectral efficiency of 5.16 bit/s/Hz. We analyze the results based on measured phase-noise characteristics of both the transmitter and the receiver combs and show that the signal quality in our experiment is currently limited by the presence of high-frequency FM noise. Our experiment represents, to the best of our knowledge, the first demonstration of coherent WDM transmission using a pair of synchronized frequency combs as a multi-wavelength source at the transmitter and as a multi-wavelength LO at the receiver.

2. Comb-based WDM coherent transmission and reception

The basic setup for a WDM transmission link with optical frequency combs used both as a multi-wavelength source for the transmitter (Tx) and as a multi-wavelength local oscillator (LO) is shown in Fig. 1. Free-running optical frequency comb sources (Tx comb, LO comb) with center frequencies $f_{\text{Tx},0}$, $f_{\text{LO},0}$ and free spectral ranges (FSR) Δf_{Tx} , Δf_{LO} supply optical carriers to the WDM transmitter and to the LO. The LO comb must be synchronized in center frequency $f_{\text{LO},0}$ and FSR Δf_{LO} to its Tx counterpart. The frequencies of the Tx comb lines Fig. 1 (Inset (1)) and of the LO comb lines Fig. 1 (Inset (2)) are denoted by

$$f_{\text{Tx},m} = f_{\text{Tx},0} + m\Delta f_{\text{Tx}}, \quad f_{\text{LO},m} = f_{\text{LO},0} + m\Delta f_{\text{LO}}, \quad (1)$$

$$m = -|M_{\text{low}}|, -(|M_{\text{low}}| - 1), \dots, -2, -1, 0, +1, +2, \dots, + (M_{\text{high}} - 1), +M_{\text{high}}.$$

The quantity m is a signed integer ranging from $M_{\text{low}} < 0$ to $M_{\text{high}} > 0$. The “inner” carriers numbered $m = -(|M_{\text{low}}| - 1), \dots, 0, \dots, + (M_{\text{high}} - 1)$ are used for coherent data transmission, whereas the “outermost” two comb lines $m = -|M_{\text{low}}|$ and $m = +M_{\text{high}}$ serve for synchronizing the LO comb frequencies to the Tx comb by minimizing the frequency offset $\delta f_0 = f_{\text{Tx},0} - f_{\text{LO},0}$ measured at line $m = 0$ and the FSR offset $\delta f_{\text{FSR}} = \Delta f_{\text{Tx}} - \Delta f_{\text{LO}}$. This synchronization ensures that all WDM channels are received within a frequency offset that is compatible with real-time intradyne reception, and that most of the receiver and digital-to-analog converter bandwidth is devoted to data reception. To this end, the beat frequencies between the “outermost” Tx comb lines M_{low} , M_{high} and their respective LO counterparts are continuously measured in a dedicated frequency synchronization setup,

$$f_{\text{Tx},M_{\text{high}}} - f_{\text{LO},M_{\text{high}}} = \delta f_0 + M_{\text{high}}\delta f_{\text{FSR}},$$

$$f_{\text{Tx},M_{\text{low}}} - f_{\text{LO},M_{\text{low}}} = \delta f_0 + M_{\text{low}}\delta f_{\text{FSR}}, \quad (2)$$

$$\delta f_0 = f_{\text{Tx},0} - f_{\text{LO},0}, \quad \delta f_{\text{FSR}} = \Delta f_{\text{Tx}} - \Delta f_{\text{LO}}.$$

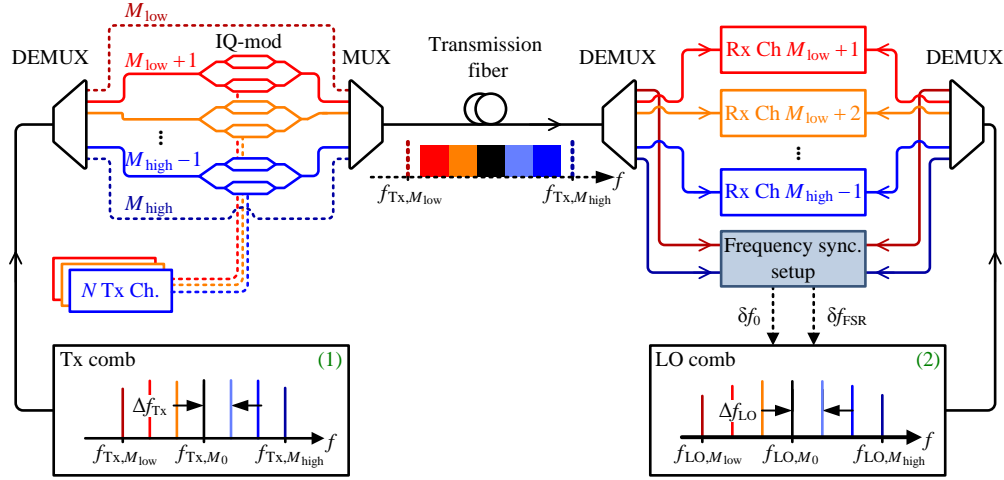


Fig. 1. Basic WDM transmission link using multi-wavelength intradyne reception. Inset (1) shows a schematic of the transmitter comb having a center frequency $f_{Tx,0}$ and an FSR Δf_{Tx} . The frequencies $f_{Tx,m}$ of the Tx comb lines are denoted by $f_{Tx,m} = f_{Tx,0} + m\Delta f_{Tx}$ where $m = -|M_{low}|, -(|M_{low}|-1), \dots, -2, -1, 0, +1, +2, \dots, +(M_{high}-1), +M_{high}$ is a signed integer ($M_{low} < 0, M_{high} > 0$). The same convention is used for the LO lines, see Inset (2). The “inner” carriers numbered $m = -(|M_{low}|-1), \dots, 0, \dots, +(M_{high}-1)$ are used for coherent data transmission, whereas the “outmost” comb lines $m = -|M_{low}|$ and $m = +M_{high}$ serve for synchronizing the LO comb frequencies to the Tx comb.

From these difference-frequency data, the FSR offset and the center frequency offset can be calculated,

$$\delta f_{FSR} = \frac{(f_{Tx,M_{high}} - f_{LO,M_{high}}) - (f_{Tx,M_{low}} - f_{LO,M_{low}})}{M_{high} + |M_{low}|}, \quad (3)$$

$$\delta f_0 = (f_{Tx,M_{high}} - f_{LO,M_{high}}) - M_{high}\delta f_{FSR}.$$

A controller circuit then adjusts the LO comb parameters $f_{LO,0}$ and Δf_{LO} for minimum offsets δf_{FSR} and δf_0 , respectively. The results obtained for this system architecture are discussed in subsequent sections.

As an alternative approach, frequency offset estimation carried out during demodulation of any two data channels can be used to estimate the center frequency and the FSR offset between the two combs instead of using the beat signals between two unmodulated carriers. This alternative method is beneficial as it will increase the spectral efficiency of the transmission link since no unmodulated Tx comb lines need to be reserved. The receiver complexity becomes slightly larger, since at least two data channels have to be simultaneously received in real time.

Another approach would be to synchronize the Tx and LO comb’s center wavelength and FSR with absolute wavelength and absolute frequency references, respectively. This approach can help maintain the combs within a given frequency grid. As such frequency references were not available to us, we decided to use the simpler approach based on unmodulated carriers.

3. Frequency comb generation

To generate the Tx and the LO comb we switch the gain of an injection-locked distributed feedback (DFB) slave laser [21]. A schematic of such a gain-switched comb source (GSCS) is depicted in Fig. 2. The DFB slave laser is gain switched by a large sinusoidal drive signal, which is generated by a voltage-controlled oscillator (VCO). The sinusoidal is superimposed

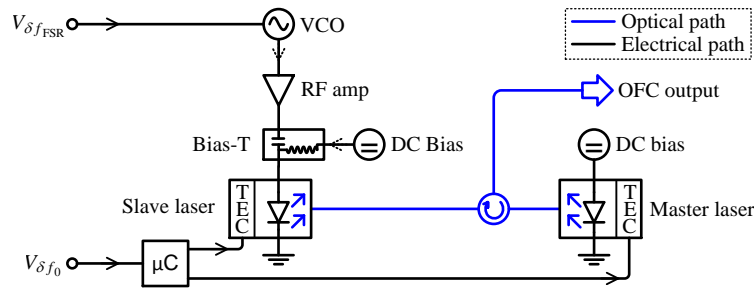


Fig. 2. Setup schematic of a tunable gain switched comb source (GSCS). A distributed feedback (DFB) slave laser is gain-switched by a large sinusoidal drive signal from a voltage-controlled oscillator that is superimposed on a DC bias current set at five times the threshold current. A master laser injects continuous-wave light into the slave via a polarization maintaining circulator thereby improving the coherence between subsequent optical pulses. This results in an optical frequency comb with low optical linewidth (100 kHz), dictated by the linewidth of the master laser. In addition, injection locking reduces the RIN of the generated comb lines. The center frequency of the resulting comb can be adjusted by temperature-tuning both master and slave with control voltage $V_{\delta f_0}$. The FSR is altered by varying the VCO frequency with control voltage $V_{\delta f_{FSR}}$.

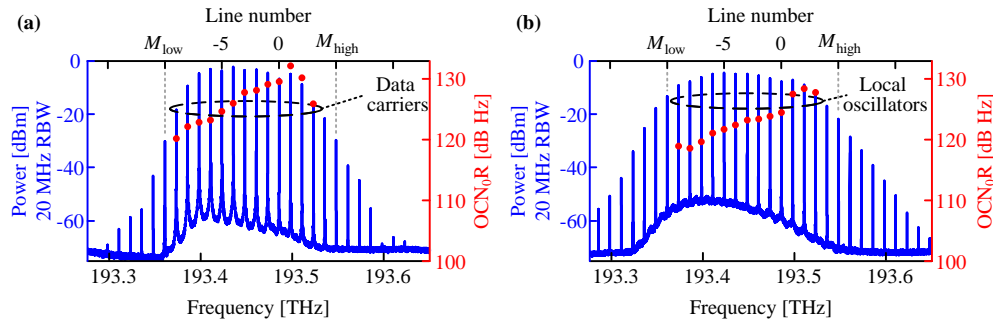


Fig. 3. Power spectra of the frequency locked combs. (a) Tx comb and (b) LO comb from the gain-switched comb sources (GSCS) recorded using a resolution bandwidth of 20 MHz. The line numbering according to Eq. (1) is shown on the upper horizontal axis. The right vertical axis gives the optical carrier-to-noise power density ratio (OCN_0R), which is marked as red filled circles for the comb lines used as data carriers and as local oscillators. It is possible to trade OCN_0R for spectral flatness of the combs [26].

on a DC bias current set at five times the threshold current of the slave laser. This leads to a pulsed output from the slave laser. A master laser injects continuous-wave light into the slave via a polarization maintaining circulator thereby establishing coherence between subsequent pulses. This leads to formation of an OFC output from the slave. The master laser also fixes the center frequency f_0 of the slave, and transfers its low optical linewidth (100 kHz) to the individual comb lines of the slave [21, 22]. In addition, injection of the master laser light into the slave reduces the RIN of the comb lines [23]. The center frequency of the resulting comb can be adjusted with a micro-controller (μC) in a predetermined fashion through temperature-tuning with thermo-electric coolers (TEC) of both the master and the slave using a control voltage $V_{\delta f_0}$. The FSR is altered (control voltage $V_{\delta f_{FSR}}$) by varying the VCO frequency [24]. Gain-switched comb sources (GSCS) can be built using monolithically integrated semiconductor lasers [25], which enables the fabrication of broadband chip-scale OFC.

Figures 3(a) and 3(b) show the measured power spectra of the Tx comb and of the LO comb used in our experiment. The resolution bandwidth (RBW) of the optical spectrum analyzer used to record the two spectra is 20 MHz. The line numbering according to Eq. (1) is displayed on the upper horizontal axis. The right vertical axis shows the optical carrier-to-

noise spectral power density ratio (OCN_0R), which is marked by red filled circles at the comb lines used as data carriers and as local oscillators. The OCN_0R is defined by the ratio of the power of the unmodulated carrier to the underlying noise power in a spectral bandwidth of 1 Hz. It is possible to trade OCN_0R for spectral flatness of the combs [26].

4. Frequency synchronization of two combs

In this section we first discuss the implementation of the synchronization of Tx and LO combs, and then report the associated experimental results.

4.1 Implementation using DSP

The setup used for synchronizing the LO comb with the Tx comb is depicted in Fig. 4(a). Note that this setup was realized using a standard off-the-shelf polarization-diverse 90° optical hybrid (PDOH) and could be simplified considerably by using dedicated hardware components. The setup consists of fiber-optic components such as erbium-doped fiber amplifiers (EDFA1, EDFA2), a polarization beam combiner (PBC), polarization controllers (PC), the PDOH, as well as electronic components such as a field-programmable gate array (FPGA) with analog-to-digital and digital-to-analog converters (ADC, DAC) and a PID controller for adjusting the FSR and the center frequency of the LO comb. Blue lines in Fig. 4 denote polarization-maintaining (PM) optical connections, red lines denote standard single-mode fibers (SSMF), and black lines denote electrical lines. The PDOH is depicted in more detail in Fig. 4(b). It consists of two polarization beam splitters (PBS1, PBS2), followed by a pair of single-polarization 90° optical hybrids (SPOH1, SPOH2) and two sets of balanced photodiodes (BD1, BD2) to extract the in-phase and the quadrature component of the beat signals of each polarization. Note that PBS1 is connected to the input port “Tx,in” of the PDOH by a polarization maintain fiber (blue), whereas PBS2 is connected to the “LO,in”-port by a standard single-mode fiber (red).

The frequency synchronization setup is fed by two comb lines at frequencies $f_{Tx,M_{low}}$ and $f_{Tx,M_{high}}$ as received from the transmitter (Tx comb lines), and by the corresponding LO comb lines at frequencies $f_{LO,M_{low}}$ and $f_{LO,M_{high}}$ extracted from the receiver (LO comb lines). The Tx comb lines arrive with an arbitrary state of polarization (SOP) in a common SSMF. These lines, after amplification by EDFA1, are adjusted in polarization to one principal axis of the PM fiber port “Tx,in” of the PDOH. This axis is aligned at an angle of 45° with respect to the main axes of PBS1, such that roughly equal-powered shares of Tx comb lines are coupled to SPOH1 and SPOH2. The LO comb lines M_{low} and M_{high} arrive on two separate SSMF in an arbitrary SOP, and are adjusted to the main axis of the PBC to superimpose them on orthogonal polarizations states at the output of the PBC. The M_{low} and M_{high} LO tones need not be phase coherent as we are using intradyne reception, where phase offset is compensated digitally. Note that the time delay between the M_{low} and M_{high} LO comb tones is much shorter than the respective coherence time between the tones such that we can always reliably estimate the FSR offset and the center frequency offset to synchronize the Tx and LO combs. The SSMF output of the PBC is then amplified and fed to the LO,in port of the PDOH, while adjusting the polarization such that the LO lines at frequencies $f_{LO,M_{low}}$ and $f_{LO,M_{high}}$ are separated by PBS2 and fed to SPOH1 and SPOH2, respectively. As a consequence, the in-phase and the quadrature component ($I_{M_{low}}$, $Q_{M_{low}}$) of the beat note between the LO and Tx comb lines at frequencies $f_{Tx,M_{low}}$ and $f_{LO,M_{low}}$ can be detected at the first set of balanced photodiodes BD1, whereas the corresponding components $I_{M_{high}}$ and $Q_{M_{high}}$ of the beat note at frequencies $f_{Tx,M_{high}}$ and $f_{LO,M_{high}}$ can be detected at the second set (BD2). Note that the beat notes of lines at $f_{LO,M_{low}}$ and $f_{Tx,M_{high}}$ and of lines at $f_{LO,M_{high}}$ and $f_{Tx,M_{low}}$ are not visible in the photocurrents due to the limited bandwidth of the photodetectors. The electrical outputs of the balanced photodiodes are sampled by a 4-

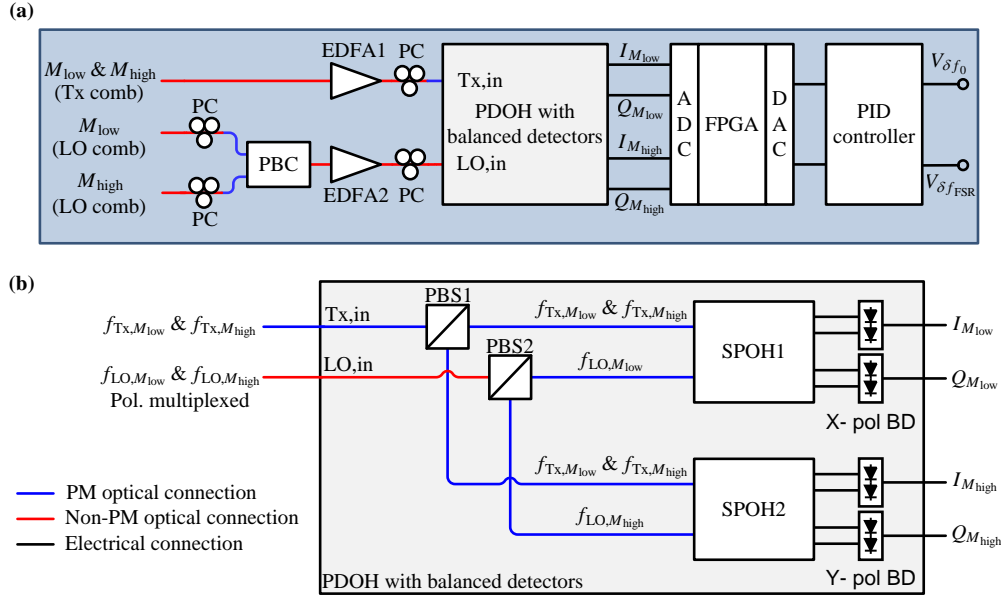


Fig. 4. Setup for frequency synchronization of two combs. (a) Overall setup: Blue lines denote polarization-maintaining (PM) optical connections, red lines denote standard single-mode fibers (SSMF), and black lines denote electrical lines. The Tx comb lines arrive with an arbitrary state of polarization (SOP) in a standard single-mode fiber (SSMF) and are first amplified by the setup. Using a polarization controller (PC), the lines are then adjusted to one principal axis of the polarization-maintaining (PM) fiber port “Tx,in” of a polarization-diverse 90° optical hybrid (PDOH), which is depicted in more detail in Fig. 4(b). The LO comb lines arrive on two separate SSMF, also with arbitrary SOP, and are adjusted to the main axes of the polarization beam combiner (PBC) to superimpose them on orthogonal polarizations states. (b) Simplified diagram of the PDOH structure: The principal axis of the PM fiber at the “Tx,in” port is aligned at an angle of 45° with respect to the main axis of a polarization beam splitter (PBS1) such that roughly equal shares of Tx comb lines are coupled to the single-polarization 90° optical hybrids SPOH1 and SPOH2. Regarding the LO signals, the polarization at the SSMF “LO,in” port is adjusted such that the LO lines at frequencies $f_{LO,M_{low}}$ and $f_{LO,M_{high}}$ are separated by PBS2 and fed to SPOH1 and SPOH2, respectively. The in-phase and the quadrature components ($I_{M_{low}}, Q_{M_{low}}, I_{M_{high}}, Q_{M_{high}}$) of the beat notes between the LO and Tx comb lines at frequencies $f_{Tx,M_{low}}, f_{LO,M_{low}}$ and $f_{Tx,M_{high}}, f_{LO,M_{high}}$ are detected by two sets of balanced photodiodes (BD1, BD2) and sampled by a 4-channel analog-to-digital converter (ADC, FMC126 from 4DSP, 1.25 GSa/s per channel). These samples are passed on to a Xilinx VC707 field-programmable gate array (FPGA) to extract the frequency differences and to control LO the comb via a PID controller.

channel analog-to-digital converter (ADC, FMC126 from 4DSP) having a sampling rate of 1.25 GSa/s per channel. These samples are passed on to a Xilinx VC707 FPGA board. A digital delay-line frequency discriminator (DLFD) [27] extracts the frequency differences $f_{LO,M_{low}} - f_{Tx,M_{low}}$ and $f_{LO,M_{high}} - f_{Tx,M_{high}}$ including the sign. The FSR offset δf_{FSR} and the center frequency offset δf_0 are then calculated by using Eq. (3). A digital-to-analog converter (DAC) on the FPGA board converts the calculated frequencies to analog voltages. These voltages serve as error signals for two PID controllers that continuously compensate the relative drifts of the LO comb via the voltages $V_{\delta f_{FSR}}$ and $V_{\delta f_0}$ which tune the FSR and the center frequency of the LO comb, see Fig. 2.

4.2 Frequency synchronization performance

To verify the synchronization of the Tx comb and the LO comb, the system response for a step-like perturbation and the system’s long-term frequency stability were investigated. Figures 5(a) and 5(b) show the responses of the center frequency offset and the FSR offset

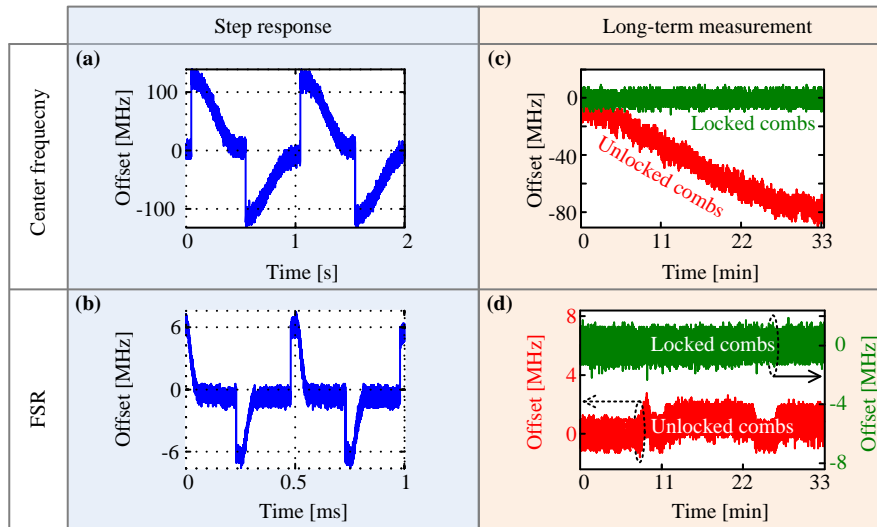


Fig. 5. Center frequency and FSR synchronization of Tx and LO combs. (a),(b) Closed-loop system response for a step like perturbation. For the case of a center frequency offset perturbation shown in (a), a 1 Hz square signal was used since the center frequency tuning speed of the LO comb is within the range of a few Hertz due to the large time constants associated with thermal tuning. For the case of an FSR offset perturbation depicted in (b), a 2 kHz square signal was used. In both cases, the frequency synchronization manages to compensate the perturbations. (c) Long-term plots of center frequency offset sampled at 50 Hz both for synchronized (“locked”) combs that are controlled by the frequency synchronization setup, and for free-running (“unlocked”) combs. (d) Long-term plots of FSR offset sampled at 50 Hz, again for locked and for unlocked combs. Two separate vertical axes are used to show the random drift in FSR of the unsynchronized combs. Plots (c) and (d) show that the control of the LO comb maintains low offsets in both center frequency and FSR.

for a closed-loop system in reaction to a step-shaped error signal. It can be seen that the LO comb tracks the center frequency offset and the FSR offset of the Tx comb. The step responses show that the center frequency tuning of the LO comb is relatively slow compared to the FSR tuning. This is expected since the center frequency is tuned by temperature, while the FSR is set by the faster reacting VCO frequency, see Fig. 2.

Long-term measurements of the center frequency offset and the FSR offset between the the LO comb and the Tx comb are shown in Figs. 5(c) and 5(d), respectively. As can be seen in Fig. 5(c), the synchronization setup maintains the long-term center frequency offset within the range of ± 10 MHz with a standard deviation of 2 MHz. Figure 5(d) shows that the FSR offset between the two combs is kept within a ± 2 MHz range having a standard deviation of less than 1 MHz. Without synchronization we observe random FSR offsets. The standard deviation of the comb offsets could be further improved if a larger averaging time is used to determine the frequency offsets for the control loop. However, this would result in a delayed response to fast frequency perturbations.

5. Tbit/s data transmission experiment

5.1 Experimental setup

The experimental setup used to characterize WDM data transmission with two synchronized GSCS is depicted in Fig. 6. In this experiment, a FSR of 12.5 GHz is used for the Tx comb. The Tx comb is first passed through a programmable filter WS1 (Finisar wavelength-selective switch) to separate the Tx comb lines into two sets. The first set consists of comb lines that are to be used as carriers for the WDM data stream. These are output through Port 1 of WS1 and further dis-interleaved into even and odd carriers. The dis-interleaver (Dis-int.)

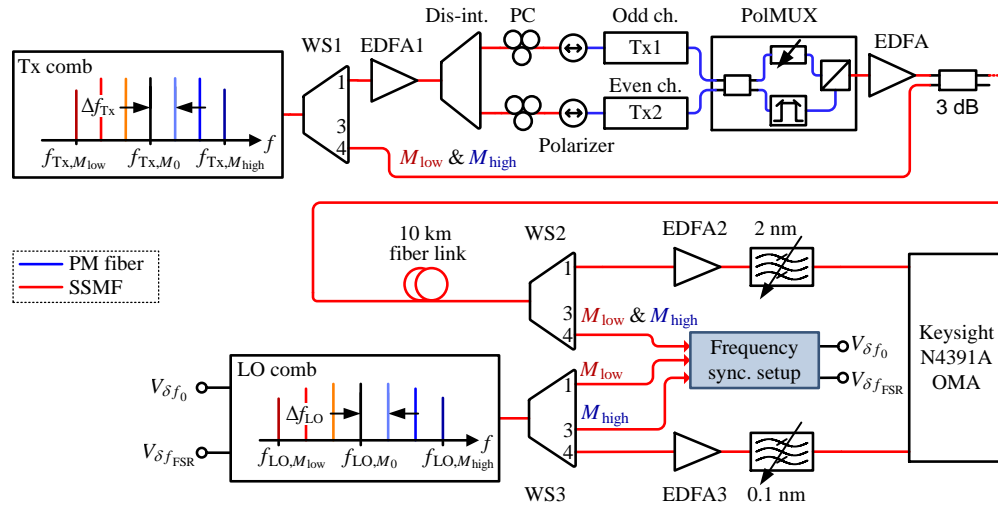


Fig. 6. Experimental setup for emulation of Tbit/s WDM transmitter and coherent receiver with multi-wavelength intradyne reception. The WDM data signal is generated by separating and independently modulating even and odd carriers. Polarization multiplexing (PolMUX) is emulated by merging decorrelated copies of the data stream onto two orthogonal polarizations. The outermost Tx comb lines M_{low} & M_{high} are selected using a programmable filter WS1 and then combined with the modulated carriers. The resulting signal is transmitted through a 10 km long fiber link to the receiver section of our setup. A programmable filter WS2 selects individual WDM channels (port 1) for detection at the receiver. In addition, it selects the M_{low} & M_{high} Tx comb lines (port 4) for use in the frequency synchronization setup. WS3 selects an LO comb line (port 4) that matches the carrier frequency of the selected WDM channel for coherent detection of the transmitted signal. WS3 is also used to select the M_{low} & M_{high} comb lines of the LO comb and routes them separately to port 1 and port 3 for use in the frequency synchronization setup. This frequency synchronization unit, see Fig. 4, synchronizes the LO comb with the Tx comb. PC: polarization controller. Tx1, Tx2: Data sources and IQ modulators.

together with two separate IQ modulators emulates WDM transmission by modulating each group of carriers with an independent pseudo-random binary data sequence of length $2^{11} - 1$.

We use either a 16QAM or a QPSK modulation format, depending on the signal quality achievable with the employed carriers. The symbol rate is 12 GBd, and the pulses are shaped according to a raised-cosine spectrum with a roll-off factor of 0.04. With an FSR of 12.5 GHz, this results in a guard band of 20 MHz between neighboring WDM channels. The frequency offset between the Tx carrier and the corresponding LO comb line needs to be maintained below this guard band value to avoid deterioration of the received signal quality. After modulation, the odd and even channels are combined by a polarization-maintaining 3 dB coupler. Polarization-division multiplexing (PDM) is then emulated by splitting the data stream into two paths and re-combining them on orthogonal polarizations with a decorrelating delay in one path and an attenuator in the other one for maintaining the same power levels. The second set of Tx comb lines at $f_{Tx, M_{low}}$ and $f_{Tx, M_{high}}$ consists of two outermost spectral lines at the edges of the Tx comb, and are output at port 4 of WS1. These lines are used for synchronization of the Tx comb's center frequency and the FSR to the corresponding quantities of the LO comb. The two outermost lines are combined with the modulated carriers by a 3 dB coupler, and all are transmitted through a 10 km long standard single mode fiber (SSMF).

At the receiver, a second programmable filter WS2 selects individual WDM channels (port 1) for detection by an optical modulation analyzer (OMA, Keysight N4391A). The two unmodulated Tx comb lines are selected and sent to port 4 of WS2 for use in the frequency

synchronization setup, see Fig. 4. A third programmable filter WS3 selects an LO comb line (port 4) that matches the carrier frequency of the selected WDM channel for coherent detection of the transmitted signal. This LO comb line is amplified and filtered with a narrow-bandwidth bandpass filter (BPF), which suppresses neighboring comb lines and out-of-band amplified spontaneous emission (ASE) noise. WS3 also selects two spectral lines of the LO comb at frequencies $f_{LO,M_{low}}$ and $f_{LO,M_{high}}$ (port 1 and port 3) for use in the frequency synchronization setup.

5.2 Data transmission performance

For demonstrating the viability of a GSCS as an LO for intradyne data reception, we extract 13 carriers from the Tx comb, modulate and transmit them, and evaluate the signal quality with the OMA. Figure 7(a) shows the spectrum of the transmitted signal captured with a resolution bandwidth (RBW) of 0.01 nm at the output of the 3 dB coupler in Fig. 6. The subscripts M_{low} and M_{high} denote the spectral lines of the Tx comb that are used for frequency synchronization. The WDM channels carry PDM-16QAM signals and are labelled according to the comb line numbering in Fig. 3. Channels -9 , -8 and $+3$ could not be used with the same modulation format because carrier power and OCN_0R were too low. However, these carriers were still sufficient for transmitting PDM-QPSK signals. Channel $+4$ was underperforming even with QPSK modulation. It could have been used as comb line M_{high} , but due to the limited steepness of the WS2 filter slope the performance of Channel $+3$ would degrade. Channel -9 , however, was not degraded, what we attribute to a better alignment of line M_{low} to the spectral pixel location of the liquid crystal-on-silicon (LCOS) matrix used in the programmable filter.

After transmission and coherent detection, a digital brick wall filter is used to limit the spectrum to our reference bandwidth 12.5 GHz. The OMA performs an adaptive equalization before determining the bit error ratio (BER) for each channel. We evaluate 500,000 bits for each WDM channel to accurately estimate the BER. Figure 7(b) shows the BER values for all 13 channels for 16QAM transmission (triangles) and for QPSK (circles). Example constellation diagrams of Channels -1 and $+3$ are shown in Fig. 7(c). BER values for two of the QPSK channels (open circles) are set at 2×10^{-6} because we did not find any error in our maximum record length of 500,000 bit. The horizontal line indicates the BER limit for forward-error correction (FEC) with an overhead of 7% [28]. We find all 13 channels to have a BER below this threshold. Hence, taking into account the 7% overhead, a line rate of 1.104 Tbit/s corresponding to a net data rate of 1.032 Tbit/s is achieved. Since 16 comb lines are utilized from the Tx and LO combs for this transmission experiment including the frequency synchronization comb lines and one idle comb line next to Channel $+3$, a net spectral efficiency (SE) of 5.16 bit/s/Hz is obtained. The SE could be improved up to 6.3 bit/s/Hz if the estimation of the frequency offsets is done from a real-time evaluation of two data channels as stated in Section 2. In the course of this experiment, the frequency synchronization setup kept the LO comb in close synchronism with the Tx comb, resulting in intradyne frequencies of less than 15 MHz for all of the evaluated data channels.

It is evident from the shape of the constellation diagrams in Fig. 7(c) that there is more angular spread of the constellation points than radial spread. This suggests a dominant phase noise contribution degrading the signal quality. It was reported in [26] that GSCS exhibit high-frequency FM-noise which may lead to such a reduction of the received signal quality. To further illustrate the effect of high-frequency FM-noise in the Tx and LO GSCS, we investigate its impact on the signal quality by two series of data transmission simulations using the commercial tool OptSim [29] with a 12 GBd 16QAM modulation. In these simulations, we do not include fiber transmission and assume an ideal receiver without any

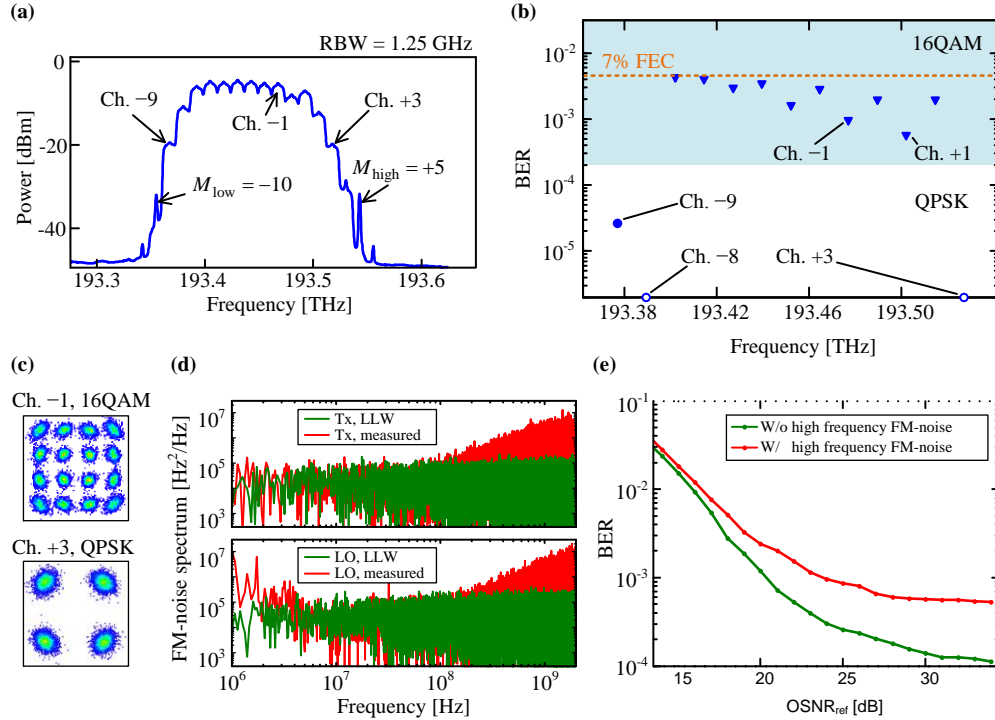


Fig. 7. Data transmission results using an LO frequency comb. (a) Tx comb spectrum measured at the output of the 3 dB coupler in Fig. 6. Lines M_{low} and M_{high} denote the Tx comb lines used for frequency synchronization. (b) Bit error ratio (BER) for all WDM channels transmitting 16QAM (\blacktriangledown) or QPSK (\bullet , \circ). All 13 channels exhibit a BER below the threshold for forward-error correction (FEC) with 7% overhead. Open symbols (\circ) indicate that no error could be found in a record length of 500,000 bit. The slight oscillations of the BER are attributed to power differences between comb lines, and to slightly different transmitter performances when encoding data on the carriers of the even and odd channels. (c) Example constellation diagrams of Channels -1 and +3. (d) Measured frequency noise spectra of Tx and LO comb lines of Channel -1 (red traces in the top and bottom subplots, respectively) featuring strong high-frequency FM noise, along with plots of simulated frequency noise spectra of idealized lasers that feature the same Lorentzian line widths (LLW) but do not exhibit high-frequency FM-noise (green). The LLW of Channel -1 Tx and LO comb lines amount to 70 kHz and 120 kHz, respectively. (e) Simulated BER vs. $OSNR_{ref}$ in a reference bandwidth of 12.5 GHz (0.1 nm) with (red) and without (green) high-frequency FM-noise. The results indicate that high-frequency FM-noise in the GSCS limits the received signal quality for high values of $OSNR_{ref}$. This limitation can be overcome by adjusting the injection locking parameters and by balancing spectral flatness and FM-noise level of the GSCS, thereby reducing high-frequency FM-noise [26].

electrical noise. The simulation results should hence give a lower boundary for the measured BER.

Tx and LO comb lines of Channel -1 are used to investigate the transmission performance in the presence of high-frequency FM-noise. The measured FM-noise spectra $S_F(f)$ of the Tx and LO comb lines of Channel -1 are depicted in Fig. 7(d) as red traces in the top and bottom subplots, respectively. $S_F(f)$ is a crucial function for evaluating the phase noise characteristics of a laser [30]. For calculating $S_F(f)$ of a comb line, we first measure the phase fluctuations $\phi_{comb}(t)$ of the comb line. To this end, the comb line and a 10 kHz line from a highly stable tunable reference laser (Keysight, N4391A) with reference phase $\phi_{ref}(t)$ are mixed, and their phase difference $\Delta\phi(t) = \phi_{comb}(t) - \phi_{ref}(t)$ is evaluated as a function of time from the intermediate frequency (IF) signal. Assuming that $\phi_{ref}(t)$ does not vary much

in comparison to $\phi_{\text{comb}}(t)$, the phase difference $\Delta\phi(t)$ is then used as an approximation of $\phi_{\text{comb}}(t)$. After obtaining $\phi_{\text{comb}}(t)$, the time increments $\Delta\phi_{\tau}(t) = \phi_{\text{comb}}(t + \tau) - \phi_{\text{comb}}(t)$ of $\phi_{\text{comb}}(t)$ for various delay times τ are estimated, and the instantaneous frequency fluctuations $f_i(t) = \Delta\phi_{\tau}(t) / 2\pi\tau$ are extracted for $\tau \rightarrow 0$. The FM-noise spectrum which is defined as the power-spectral-density (PSD) function of the instantaneous frequency fluctuation $f_i(t)$ is then calculated as $S_F(f) = |\text{FFT}\{f_i(t)\Delta t\}|^2 / T$, where FFT represents the fast Fourier transform. The quantity Δt is the sampling interval, and T is the total sample duration.

In the first series of simulations, OptSim laser models were made to have similar FM-noise characteristics as the actually measured Tx and LO comb lines of Channel -1. We did so by phase modulating the light emitted from the ideal OptSim laser models with the measured phase fluctuations $\phi_{\text{comb}}(t)$ of the Tx and LO comb lines of the channel under consideration. The resulting signals from the laser models emulate the actual comb lines, and are then used as the signal and LO tones for a transmission experiment simulation. The obtained dependence of BER for a 16QAM signaling on the optical signal-to-noise ratio (OSNR_{ref}) is shown by the red trace in Fig. 7(e). Here, the OSNR_{ref} is defined as the ratio of total signal power and noise power measured in a reference bandwidth of 12.5 GHz (0.1 nm).

In the second series of simulations, Lorentzian lineshape laser models without high-frequency FM-noise were used as provided by OptSim. For a realistic connection to the measured data, the Lorentzian linewidths (LLW) of the Tx and the LO comb lines in the simulation are chosen as $\text{LLW} = 2\pi \cdot S_F^{\text{white}}(f)$, where $S_F^{\text{white}}(f)$ is the flat FM-noise component in the low-frequency region of the measured FM-noise spectra $S_F(f)$ of Channel -1 [30]. Using this procedure, the linewidth in the simulation is set to be 70 kHz (120 kHz) for the Tx (LO) laser. The FM-noise spectra of the OptSim Lorentzian lineshape laser models are also depicted as green traces in Fig. 7(d). As expected, the BER is better for the simulated Lorentzian lineshapes as compared to the sources which feature additional high-frequency FM-noise, see green trace in Fig. 7(e). The difference becomes more pronounced as the OSNR_{ref} level increases.

In our experiment, a direct measurement of the OSNR_{ref} was not possible due the densely packed channel spectra that made it impossible to measure the noise background of the data signal. Hence, a direct comparison of the simulation results to the measured BER is difficult. However, in the presence of high-frequency FM noise, the simulated BER of approximately 4×10^{-4} in the limit of high OSNR_{ref} compares well to the best experimentally obtained BER of 6×10^{-4} observed for Channel +1, see Fig. 7(b). This indicates that high-frequency FM-noise in GSCS limits the received signal quality, indeed. The limitations could be overcome by adjusting the injection locking parameters and balancing spectral flatness and FM-noise level of the GSCS which leads to a reduction of high-frequency FM-noise [26].

5.3 Scalability and power consumption

As it is not possible to generate a significantly larger number of lines from our GSCS, we will need to use multiple transmitter/receiver groups to further increase the overall transmission capacity. This can be done by integrating multiple GSCS on one chip [25].

In general, frequency combs have the advantage of a greatly simplified wavelength stability of the individual carriers as the control of center frequency and FSR is sufficient to stabilize and synchronize all Tx and Rx comb lines. This advantage becomes particularly important for large channel counts. Of course, nothing comes for free, and the power per line decreases as the number of lines increases, which in our experiment requires an additional EDFA before the modulator (EDFA1 in Fig. 6). Taking this amplifier into account, we obtain between 10 dBm and 14 dBm of optical power per tone, which compares well to the optical output power of common integrated tunable laser assemblies (ITLA) [31]. At the same time, the electrical power consumption of an integrated GSCS is estimated to be about 2 W per

line, taking into account a power consumption of 10 W for the GSCS [13] and an additional 8 W for the EDFA [32]. This total power consumption is already slightly below that of a commercial ITLA [31]. The advantages of using frequency combs become even more pronounced when moving to higher channel counts. We have recently shown WDM transmission using approximately 100 carriers derived from a so-called Kerr soliton comb [14, 33]. For this device, we estimate an overall power consumption of less than 1 W per line, including all EDFA required to boost the comb to optical power levels of about 10 dBm per line. We hence are convinced that the concept of using frequency combs is an attractive option to realize highly scalable optical multi-wavelength sources for WDM transmission.

6. Summary

We demonstrate that a GSCS is suitable to serve as a multi-wavelength local oscillator (LO) for intradyne reception of WDM signals. Center frequency and FSR of the LO comb are synchronized to the transmitter frequency comb. We demonstrate the viability of the concept in a proof-of-principle experiment by transmitting a net aggregate data rate of 1.032 Tbit/s through a 10 km long SSMF with a net spectral efficiency of 5.16 bit/s/Hz. Using simulations based on measured phase-noise characteristics, we show that the performance is limited by the presence of high-frequency FM-noise which, however, can be decreased by a proper parameter optimization of the comb sources.

Funding

European Research Council (ERC) Starting Grant ('EnTeraPIC', 280145); the EU project BIG PIPES (619591); Alfried Krupp von Bohlen und Halbach Foundation; Helmholtz International Research School for Teratronics (HIRST); Karlsruhe School of Optics & Photonics (KSOP); Erasmus Mundus Joint Doctorate program EUROPHOTONICS (159224-1-2009-1-FR-ERA MUNDUS-EMJD); Deutsche Forschungsgemeinschaft (DFG) (1173).

Acknowledgments

We acknowledge an unknown referee for pointing out the possible use of absolute frequency and wavelength references, end of Sect. 2. We further acknowledge support by the Open Access Publishing Fund of Karlsruhe Institute of Technology (KIT).